DeepfakeMAE: Facial Part Consistency Aware Masked Autoencoder for Deepfake Video Detection

Juan Hu [1], Xin Liao [1]*, Difei Gao [2], Satoshi Tsutsui [3], Zheng Qin [1], Mike Zheng Shou[2]

[1] The College of Computer Science and Electronic Engineering, Hunan University, China
[2] Show Lab, National University of Singapore, Singapore
[3] ROSE Lab, Nanyang Technological University, Singapore

arXiv:2303.01740v1 [cs.CV] 3 Mar 2023

Abstract

Deepfake techniques have been used maliciously, resulting in strong research interests in developing Deepfake detection methods. Deepfake often manipulates the video content by tampering with some facial parts. However, this manipulation usually breaks the consistency among facial parts, e.g., Deepfake may change smiling lips to upset, but the eyes are still smiling. Existing works propose to spot inconsistency on some specific facial parts (e.g., lips), but they may perform poorly if new Deepfake techniques focus on the specific facial parts used by the detector. Thus, this paper proposes a new Deepfake detection model, Deepfake-MAE, which can utilize the consistencies among all facial parts. Specifically, given a real face image, we first pretrain a masked autoencoder to learn facial part consistency by randomly masking some facial parts and reconstructing missing areas based on the remaining facial parts. Furthermore, to maximize the discrepancy between real and fake videos, we propose a novel model with dual networks that utilize the pretrained encoder and decoder, respectively. 1) The pretrained encoder is finetuned for capturing the overall information of the given video. 2) The pretrained decoder is utilized for distinguishing real and fake videos based on the motivation that DeepfakeMAE's reconstruction should be more similar to a real face image than a fake one. Our extensive experiments on standard benchmarks demonstrate that DeepfakeMAE is highly effective and especially outperforms the previous state-of-the-art method by 3.1% AUC on average in cross-dataset detection.

1. Introduction

The innovation of Generative Adversarial Networks (GANs) has led to the emergence of Deepfake, defined as a set of methods that synthesize human faces based on AI algorithms [46]. Despite its spectacular potential in film, art,

---
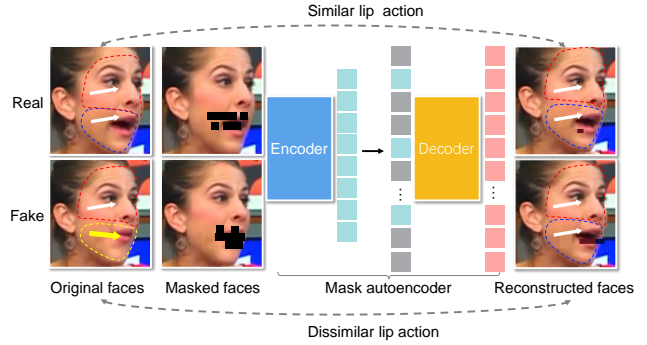*Corresponding author: Xin Liao.

Figure 1. We reconstruct faces from masked fake and real faces by utilizing our proposed DeepfakeMAE. We assume that Deepfake videos often lack the consistency among facial parts (or *facial part consistency*) and that DeepfakeMAE can reconstruct better for real faces than that of fake faces. For example, manipulating lips will make the lips' appearance inconsistent with other facial parts. As a result, the lips restored by DeepfakeMAE are closer to the original in the real image than in the fake image. We utilize these characteristics for detecting Deepfake videos.

and entertainment, the malicious use of Deepfake threatens the psychological security [47] of individuals, the public, and even nations, motivating Deepfake detection.

Many Deepfake detection methods have been proposed, which can be broadly classified into two categories: those based on implicit clues and those based on explicit clues. Methods based on implicit clues [1, 2, 25, 34, 37, 38, 40, 50] often use supervised learning to classify fake or real without explicitly designing clues to detect Deepfake videos, which makes it harder to tell what kind of clues are used for detection due to the black-box nature of deep learning. Methods based on explicit clues [3, 4, 12, 14, 15, 18, 23, 24, 26, 29, 32, 33, 36, 45, 48, 51] design some specific clues to detect Deepfake videos. For example, lips movement [15] has been shown to achieve state-of-the-art generalization performance to unknown manipulated patterns. Nevertheless, diverse and rapidly advancing Deepfake methods leave dif-

ferent forgery traces. Hence, detection methods that depend on a specific facial part can have a weakness due to their dependence on it. In other words, methods that use specific clues may perform poorly if the clue is exploited by attackers. Moreover, in the real world scenario, the given video may be generated by unknown manipulation techniques, which can cause the performance to drop [29,45,50] when detecting forgeries outside the training dataset. This motivates us to develop a method that does not use any manually designed clues or specific Deepfake patterns, but also that does not simply perform supervised learning to classify fake or real.

Deepfake methods often are hard to generate expressive faces as in the real world because the generation process ignores the consistency among facial parts (or *facial part consistency*) that exists in real faces [12–14, 48, 51]. The inconsistency of fake videos not only appears in specific facial parts like lips, but could happen among all facial parts. *The core idea of this paper is that it is not easy to generate videos with perfect facial consistency, but getting a model that can restore a masked face image while maintaining consistency is much easier and possible*, because the reconstruction model could always be stronger than generative models. The reconstruction model can then be used as a probe to detect the model. Specifically, since the fake one breaks the facial consistency, the reconstruction process of a fake image will correct the non-consistency parts, resulting in differences between the original and reconstructed images. In contrast, the original and the reconstructed faces of a real image will remain the same. For example, in Figure 1, the fake face of FaceForensics++ dataset [37] has lips tampered to not be upward, lacking consistency with other facial parts because the cheek and eyes parts are upward. As a result, the reconstructed image corrects such a fault. Moreover, by designing flexible masking strategies, the reconstruction model is expected to learn general facial part consistency among all facial parts.

Thus, following the above idea, this paper proposes a two-stage model, consisting of DeepfakeMAE pretraining and finetuning for Deepfake detection in unknown domains (*i.e.* the types of fake that are not used in training). Specifically, the goal of the first stage is *pretraining a model to capture the consistency among all facial parts*. Inspired by [16], we propose a new self-supervised pretraining method based on masked autoencoder, named DeepfakeMAE. Compared to MAE [16], which randomly masks the most parts of the image, DeepfakeMAE introduces a simple masking strategy conditioned on face feature points to randomly mask the region of a facial part at one time, as shown in Figure 1. The autoencoder can thus better learn the facial part consistency by reconstructing the missing pixels.

The goal of the second stage is *utilizing the pretrained*

model to distinguish a real and fake video. Specifically, it finetunes the representation from the first stage, so that it has the better discriminability of real and fake ones and the better domain generalization on diverse Deepfake patterns. To do so, we design two sub-networks. The first branch (Fig.2-a) is Finetuning Network that takes multiple video frames and finetunes the model to classify real videos and fake videos. Using the trained encoder of the first stage to extract characteristics, the model can learn the difference between real videos and fake videos with respect to the consistency of facial parts. The second branch (Fig.2-b) is Mapping Network, which employs the trained decoder of the first stage to reconstruct faces. By developing a mapping network, the branch can map original real faces into its DeepfakeMAE's reconstruction, but fail to map fake faces into its DeepfakeMAE's reconstruction. By minimizing the mean squared error (MSE) loss between reconstructed faces and mapped faces, the model amplifies inconsistencies in fake faces and consistencies in real videos. Furthermore, to explicitly promote the generalization to unseen DeepFake patterns, we use meta-learning, where the different types of Deepfake videos are split into Meta-train and Meta-test in the training phase.

Contributions.

1. We propose DeepfakeMAE for the Deepfake detection that can learn to utilize the consistences among all facial parts.
2. To develop a model that can generalize to unseen Deepfake patterns, we introduce a two-stage strategy, where the first stage uses real images only and learns the representation unspecific to any Deepfake or any facial part, and the second stage learns a more robust representation that maximizes the discrepancy between real faces and fake faces.
3. Extensive experiments on benchmark datasets, including FaceForensics++ [37], Celeb-DF [28], WildDeepfake [52], and DFDC [7] show that DeepfakeMAE achieves excellent performance under various metrics.

2. Related Work

2.1. Deepfake Synthesis Methods

Li et al. [28] break down the Deepfake synthesis methods into two generations. First-generation methods include Face2Face [43], FaceSwap [9], NeuralTextures [42], and DeepFakes [6]. Face2Face synthesizes target faces by warping source faces. FaceSwap applies the rendered model and color correction to swap the face region. NeuralTextures trains a model to learn neural texture features of target videos and perform facial reenactment. DeepFakes is based on two autoencoders and a decoder to generate fake videos. First-generation methods have some known issues, such as color mismatches, temporal flickering, and incorrect

face boundaries. The second-generation methods improve the quality over the previous methods. Specifically, Celeb-DF [28] applied an algorithm to reduce boundary artifacts and improve inter-frame continuity. Dolhansky at al. [7] increase the perceptual quality of Deepfake videos using additional GAN models (NTH [49], FSGAN [35], Style-GAN [21], etc.).

These diverse synthesis methods leave different tampered traces and cause biased data distributions, making it challenging to detect Deepfake videos in unknown domains. In this paper, we utilize the videos from public datasets that contain the aforementioned two generations' methods.

2.2. Deepfake Detection Methods

Methods based on implicit clues mainly perform supervised learning to classify fake or real. The early method [1] develops Mesonet to extract mesoscopic properties. To amplify artifacts and suppress the high-level face content, Masi et al. [31] introduce a two-branch recurrent network for isolating manipulated faces. Zi et al. [52] propose ADDNets with attention mechanisms for advanced Deepfake detection. To improve the robustness, Cao et al. [2] design an end-to-end reconstruction network with an attention module to guide the model to focus on tampered traces.

Methods based on explicit clues leverage various specific information to improve detection performance. Signal clues such as frequency information [29, 36], local textures [27], and biological features [5] are employed to distinguish Deepfake videos from real videos. Semantic clues like emotion features between audio and visual [32], temporal inconsistencies [13, 19], lips information [15] exhibit remarkable progress in Deepfake detection. Sun et al. [41] propose an LTW network to balance the robustness of the model by combining multiple domains. To develop a generalizable Deepfake detector, Chen et al. [4] design a synthesizer and adversarial training framework and enforce the framework to predict forgery configurations.

These methods achieve promising results on current benchmarks, but they rely on specific clues. With the emergence of new Deepfake techniques, specific clues extracted by detection methods may be circumvented by purposely training during the synthesis of fake videos. Unknown Deepfake patterns leave complex manipulated traces rather than foreseeable specific features, which motivates us to further explore developing detectors for unknown domains without using specific clues. Hence, we propose a self-supervision method that reconstructs randomly masked faces to learn robust features that are not specific to any facial parts, promoting the model to learn the consistencies of facial parts.

2.3. Masked Autoencoder Methods

The emergence of the masked autoencoder (MAE) [16] has greatly influenced our community due to its simplicity and effectiveness. Thereafter, extent MAE [10], Video-MAE [44], and ConvMAE [11] are proposed to learn strong representations. These MAE methods are based on an asymmetric encoder-decoder architecture. The extent MAE [10] mainly extends MAE to spatiotemporal representations. VideoMAE [44] develops a customized design of tube masking based on MAE. ConvMAE [11] introduces a convolution structure in MAE. Although they are relatively small modifications, the performance of various downstream tasks has been greatly improved.

MAE [16] is designed for pretraining Vision Transformers (ViT) rather than for Deepfake detection. Unlike MAE that randomly masks patches, we modify the masking strategy not to lose the semantics of the facial parts, and so that it can enforce the autoencoder to learn the representation that has the consistency of facial parts.

3. Method

This section presents the details of DeepfakeMAE for Deepfake video detection. To better extract robust features for unknown Deepfake patterns, this method utilizes a facial masked autoencoder for feature learning. Furthermore, the proposed method utilizes dual networks to detect differences between real videos and fake videos using the trained model of the facial masked autoencoder. Specifically, the proposed method is composed of two stages: (1) MAE for Consistency Learning stage, (2) Dual Networks for Discrepancy Learning stage, as shown in Fig. 2. The first stage trains the model to learn the facial part consistencies of real faces. The second stage is composed of two branches: Fine-tuning Network and Mapping Network.

3.1. MAE for Consistency Learning Stage

In this stage, we customize MAE [16] and its masking strategy with minimal but effective modifications, so that the model can learn generic facial part consistency features and can also prevent over-fitting to specific forgery patterns.

Masking strategy tailored to learn the consistent face representation. We customize the original masking strategy from MAE [16] and design a facial part masking strategy to ensure that the model can learn the consistencies of all facial parts. We show the pseudo-code in Algorithm 1, which takes the inputs of real videos' faces and outputs the masked faces. The original MAE [16] masks random patches of the input image, but the same strategy is not suitable for our DeepfakeMAE for the following reasons. First, because each facial part is a semantic entity for Deepfake detection, simple random masking without caring the

First Stage: MAE for Consistency Learning

Second Stage: Dual Networks for Discrepency Learning

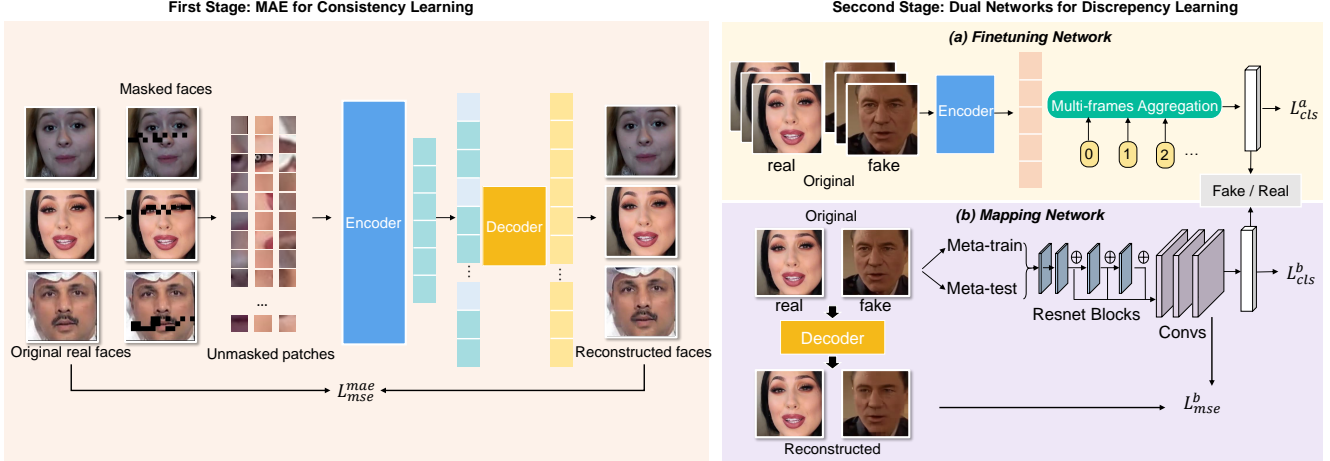*(a) Finetuning Network*

(b) Mapping Network

Figure 2. Pipeline of the propose DeepfakeMAE. In the first stage (Sec. 3.1), DeepfakeMAE learns general facial part consistencies of real faces by developing the masked autoencoder. In the second stage, DeepfakeMAE performs *(a) Finetuning Network* (Sec. 3.2.1) and *(b) Mapping Network* (Sec. 3.2.2) to leverage the pretrained DeepfakeMAE model for better capturing the discrepancy between real videos and fake videos.

semantics can destroy the consistency of each facial part. If the consistency is destroyed, it is difficult for the model to learn correct facial part consistency features. Hence, our proposed masking strategy explicitly distinguishes three facial parts, i.e., eyes, cheek & nose, and lips, facilitating the model to focus on the consistencies among these facial parts. Second, the original masking strategy with a high masking ratio would make it too difficult to restore the original appearance without artifacts or distortions. Thus, we proposed a masking strategy that utilizes a relatively low masking ratio so that the model can reconstruct the original faces more accurately. We discuss more about the masking ratio in Section 4.4.

Network Architecture. Our masked autoencoder is based on an asymmetric encoder-decoder architecture [16]. The encoder is a ViT [8] but applied only on unmasked patches. The decoder is a series of Transformer blocks but applied on both mask tokens and encoded features of unmasked patches.

Reconstruction. The masked patches of faces are dropped in the processing of the encoder, leaving the unmasked areas. In this way, the decoder predicts the missing facial part based on the unmasked areas. The reconstruction quality of masked patches is calculated with the MSE loss function L_{mse}^{mae}. If the model learns consistencies among facial parts, the loss between the reconstructed patches and the input patches should decrease. Our facial part masking strategy makes each part selected randomly, which enforces the model to learn the representation unspecific to any facial part. Furthermore, because this stage only uses real videos and does not use any Deepfake videos, it can prevent the model from over-fitting to any specific tampering pattern.

Algorithm 1: Masking process of facial parts

Input: Real faces: F, Mask ratio: M_r;
Output: Masked real faces;

1   Detect 68 keypoints in faces;
2   Partition image patches based on keypoints into three sets;
3   Eyes patches $\in \{(0,0) \rightarrow$ the landmark of $17^{th}\}$, and Nose & cheek patches $\in \{$end of eyes patches $\rightarrow$ the landmark of $16^{th}\}$, and Lips patches $\in \{$end of Nose & cheek patches $\rightarrow$ the last patches of $F\}$;
4   $M_i, i \in [1, 2, 3]$, which indicates patches of eyes, nose & cheek, and lips region respectively;
5   Random select one set of patches;
6   Random mask M_r portion of selected set;

After the training of the first stage, the pretrained DeepfakeMAE model is obtained.

3.2. Dual Networks for Discrepancy Learning Stage

In this stage, we leverage the well-trained DeepfakeMAE model from the first stage so that the model can better capture the discrepancy between real and fake videos, using two branches: (a) Finetuning Network, and (b) Mapping Network. By adopting the well-trained model of the first stage, the two branches are combined to detect Deepfake videos with the separate training.

3.2.1 Finetuning Network

Finetuning Network uses both real videos' frames and Deepfake videos' frames with a cross-entropy loss L_{cls}^a to

extract the discrepancy between real videos and fake videos. Firstly, we extract frames from real and Deepfake videos, and crop faces from frames. Thereafter, original real faces and original fake faces with full sets of patches are put into the well-trained encoder of the first stage. To aggregate the information of multi-frames, we average the outputs of 5 frames, using the last layer of the encoder.

Since the first stage learns the facial part consistency of real videos, the well-trained encoder of DeepfakeMAE can extract consistency features of real videos. For fake videos, because the consistency is destroyed, the features extracted from the encoder can be different from that of real videos. Finetuning Network will amplify the discrepancies between fake and real videos, which improves the detection performance.

3.2.2 Mapping Network

Data split strategy. To avoid over-fitting to specific Deepfake patterns, we use meta-learning [20] and randomly divide the training data into Meta-train set and Meta-test set, where fake faces in Meta-train and Meta-test have different manipulated patterns. Since this branch requires different types of faces rather than a large number of faces, we utilize a single frame to train the branch for reducing memory consumption.

Network Architecture. We utilize the first convolutional layer of ResNet-18 [17]. The first three residual blocks of ResNet-18 are employed, and the outputs of these residual blocks are concatenated. The concatenated outputs are fed into three convolutional layers for face mapping. The dimensions of the mapped faces are $56 * 56 * 3$. We minimize the MSE loss L_{mse}^b between the mapped faces and the reconstructed faces of the input. Ultimately, a fully connected (FC) layer is utilized for classifications. We also minimize the binary cross-entropy L_{cls}^b between the branch output and the video label.

Meta-train phase. For each epoch, a sample batch is formed with the same number of fake videos and real videos to construct the binary detection task. The Meta-train phase performs training by sampling many detection tasks, and is validated by sampling many similar detection tasks from the Meta-test. Thereafter, the parameters of Meta-train phase can be updated. To select the best gradient step, we set a reference set, denoted as T_i^{ref}. We utilize each gradient step to calculate the accuracy of T_i^{ref}. The parameters with the highest accuracy are selected as the final updated parameters. Ultimately, the Meta-train phase utilizes the updated parameters to calculate the Meta-train loss.

Since the first stage learns the consistencies of all facial parts in real videos, the model should output the inconsistent representations when the consistency of a face is destroyed. In other words, the fake faces reconstructed from the trained decoder of the first stage should expose incon-

sistencies. Optimizing L_{mse}^b allows the mapped faces of real videos to be constrained by the consistency of reconstructed real faces, while the mapped faces of fake videos are constrained by the inconsistency of reconstructed fake faces. Ultimately, the model can observe that the real faces maintain consistencies in facial parts, while the fake ones' consistencies are broken.

Meta-test phase. The goal of Meta-test phase is to enforce a classifier that performs well on Meta-train and can quickly generalize to the unseen domains of Meta-test, so as to improve the cross-domain detection performance. Specifically, we sample a batch in Meta-test domain and another batch in the Meta-train domain to concatenate to a random array. Then, we use the random array and the updated parameters to compute the Meta-test loss of L_{cls}^b and L_{mse}^b.

Detection loss. The final loss function of Mapping Network is:

$$L^b = (\lambda^{cls} \cdot L_{cls}^b + \lambda^{mse} \cdot L_{mse}^b)_{Meta-train}$$
$$+ (\lambda^{cls} \cdot L_{cls}^b + \lambda^{mse} \cdot L_{mse}^b)_{Meta-test}. \quad (1)$$

which combines the Meta-test loss of L_{cls}^b and L_{mse}^b and Meta-train loss of L_{cls}^b and L_{mse}^b to achieve joint optimization.

4. Experiment

4.1. Experimental Setup

Datasets. Four public Deepfake videos datasets, i.e., FaceForensics++ [37], Celeb-DF [28], WildDeepfake [52], DFDC [7] are utilized to evaluate the proposed method and existing methods. FaceForensics++ is made up of 4 types manipulated algorithms: DeepFakes [6], Face2Face [43], FaceSwap [9], NeuralTextures [42]. Moreover, 4000 videos are synthesized based on the 4 algorithms. These videos are widely used in various Deepfake detection scenarios. Celeb-DF contains 5639 videos that are generated by an improved DeepFakes algorithm [28]. The tampered traces in some inchoate datasets are relieved in Celeb-DF. WildDeepfake consists of 707 Deepfake videos that were collected from the real world. The real world videos contain diverse scenes, facial expressions, and forgery types, which makes the datasets challenging. DFDC is a large-scale Deepfake detection dataset published by Facebook.

Implementation details. In the first stage, the masking ratio, batch size, patch size, and input size are set as 0.5, 8, 16, 224, respectively. The AdamW [30] optimizer with an initial learning rate $1.5 \cdot 10^{-4}$, momentum of 0.9 and a weight decay 0.05 is utilized to train the model. In the second stage, the Finetuning Network utilizes the AdamW optimizer with an initial learning rate $1 \cdot 10^{-3}$ to detect videos. The SGD optimizer is used for optimizing the Mapping Network with the initial learning rate 0.1, momentum of 0.9, and weight decay of $5 \cdot 10^{-4}$. We use FFmpege [22] to extract frames

Table 1. Cross-dataset generalization. Comparisons of the cross-dataset evaluation (AUC (%)) between DeepfakeMAE and baseline methods on Celeb-DF, WildDeepfake, and DFDC datasets when trained on FaceForensics++.

Method	Testing datasets			
	Celeb-DF	WildDeepfake	DFDC	Avg
FWA [27]	69.5	68.2	67.3	68.3
ADDNet [52]	60.9	54.2	65.9	60.3
Face X-ray [24]	79.5	77.3	65.5	74.1
CNN-aug [45]	75.6	*	72.1	*
MultiAtt [50]	67.4	65.7	71.0	68.0
SPSL [29]	76.9	70.9	66.2	71.3
LTW [40]	64.1	*	69.0	*
LipForensics [15]	82.4	78.1	73.5	78.0
FInfer [18]	70.6	69.5	70.4	70.2
HCIL [14]	79.0	*	69.2	*
Chen et al. [4]	79.7	*	*	*
RECCE [2]	68.7	64.3	69.1	67.4
DeepfakeMAE	**86.3**	**81.8**	**75.2**	**81.1**

Table 2. Cross-manipulation generalization. Comparisons of the cross-manipulation evaluation (AUC (%)) between DeepfakeMAE and baseline methods on each forgery type of FaceForensics++ when trained on one type. DeepFakes, FaceSwap, Face2Face, NeuralTextures are represented as DF, FS, F2F, and NT, respectively.

Method	Train	F2F	FS	NT	Avg
Freq-SCL [23]	DF	58.9	66.9	63.6	63.1
MultiAtt [50]		66.4	67.3	66.0	66.6
RECCE [2]		70.7	74.3	67.3	70.8
DeepfakeMAE		**86.6**	**77.2**	**69.4**	**77.7**

Method	Train	DF	FS	NT	Avg
Freq-SCL [23]	F2F	67.6	55.4	66.7	63.2
MultiAtt [50]		73.0	65.1	71.9	70.0
RECCE [2]		76.0	64.5	**72.3**	71.0
DeepfakeMAE		**88.9**	**71.4**	55.1	**71.8**

Method	Train	DF	F2F	NT	Avg
Freq-SCL [23]	FS	75.9	54.6	49.7	60.1
MultiAtt [50]		82.3	61.7	54.8	66.3
RECCE [2]		**82.4**	64.4	**56.7**	67.8
DeepfakeMAE		80.0	**80.9**	47.3	**69.4**

Method	Train	DF	F2F	FS	Avg
Freq-SCL [23]	NT	79.1	74.2	54.0	69.1
MultiAtt [50]		74.6	80.6	60.9	72.0
RECCE [2]		78.8	**80.9**	**63.7**	**74.5**
DeepfakeMAE		**85.7**	63.4	62.4	70.5

from videos. The `dlib` [39] is utilized to detect 68 facial landmarks. We randomly mask facial parts according to Algorithm 1 for the training of the first stage. In the second stage, we use `dlib` to extract faces. These faces are fed into the model without mask patches.

4.2. Generalization to Unknown Domains

We design a detector that automatically learns consistencies among all facial parts, which enforces the model to learn robust features for the detection of unknown domains. To test this point, we simulate unknown domains Deepfake detection scenarios below.

Cross-dataset generalization. To evaluate the generalization of DeepfakeMAE, we construct cross-dataset experiments. Since videos of different datasets possess relatively dispersed distributions, cross-dataset experiments can simulate unknown domains detection. Specifically, we implement the cross-dataset experiments by training the model on FaceForensics++ with all 4 types of videos, but testing on other datasets, i.e., Celeb-DF, WildDeepfake, DFDC.

Table 1 shows that DeepfakeMAE achieves a satisfactory generalization to unseen datasets surpassing previous methods. It also outperforms the previous state-of-the-art method, LipForensics [15], by 3.9% AUC on Celeb-DF, by 3.7% AUC on WildDeepfake, by 1.7% AUC on DFDC. We note that LipForensics [15] focuses on the features of the lips area, but the proposed DeepfakeMAE enforces the model to automatically learn the consistency features of all

parts. The performance in Table 1 provides evidence that the random mask of all facial parts is important for generalization. When testing on WildDeepfake and DFDC, the detection performance of most methods is significantly degraded. This is possibly due to the domain shift caused by different types of fakes. Specifically, videos in WildDeepfake are collected in the wild enriching the video types. Videos in DFDC datasets are generated by diverse Deepfake technologies that are different from FaceForensics++. The enormous differences between training domain and testing domain make it challenging to improve cross-dataset detection performance. Nonetheless, the proposed DeepfakeMAE manages to reach 81.8% and 75.2% AUC on WildDeepfake and DFDC.

Cross-manipulation generalization. We also carry out cross-manipulation experiments to assess the generalization to unknown manipulation patterns. Videos in FaceForensics++ are generated from 4 forgery technologies. Following RECCE [2], we select each type of videos for training and the remaining three types of videos for testing. In

Table 3. Comparisons of the Intra-dataset evaluation (AUC (%)) between DeepfakeMAE and baseline methods on FaceForensics++ (HQ).

Method	DF	FS	F2F	NT	Avg
Xception [37]	98.9	99.6	98.9	95.0	98.1
ADDNet [52]	92.1	92.5	83.9	78.2	86.7
S-MIL [25]	98.6	99.3	99.3	95.7	98.2
STIL [12]	99.6	**100**	99.3	95.4	98.6
HCIL [14]	**100**	**100**	99.3	**96.8**	**99.0**
DeepfakeMAE	99.6	99.4	**99.4**	96.3	98.7

Table 4. Ablation study - The cross-dataset detection performance (AUC %) of different masking ratios (25%, 50%, 75%) on Celeb-DF, WildDeepfake, and DFDC datasets.

Dataset	25%	50%	75%
Celeb-DF	85.1	**86.3**	84.6
WildDeepfake	80.6	**81.8**	79.9
DFDC	74.4	**75.2**	73.7

this way, the meta-learning mode is different from that of the cross-dataset experiments that split training data according to the tampered types. Since there is only one type of videos for training in cross-manipulation experiments, we randomly split the training data into Meta-train and Meta-test with $8 : 2$.

Results in Table 2 illustrate that DeepfakeMAE outperforms previous methods in many scenarios. When the model is trained on DeepFakes and tested on other three types of videos, DeepfakeMAE improves the performance by 6.9% on average. Besides, our method has a little bit more difficulty in detecting the Deepfake videos using neuraltextures than the other methods. NeuralTextures learns specific neural texture features [42] to train a model to generate faces leaving specific artifacts. On the contrary, the proposed DeepfakeMAE focuses on unspecific features, which might be the reason why our method does not generalize well on NeuralTextures.

4.3. Intra-dataset Detection Performance

To comprehensively assess the proposed Deepfake-MAE, we compare DeepfakeMAE with the state-of-the-art methods in the scenario of intra-dataset detection. Specifically, we conduct experiments on 4 subsets of FaceForensics++ (HQ). The training data and testing data of intra-dataset experiments are from the same subset of FaceForensics++ (HQ). Table 3 shows the results that most methods perform well in intra-dataset detection. While Deepfake-MAE achieves the best intra-dataset detection performance on Face2Face, HCIL [14] achieves the best intra-dataset detection performance on average. Although DeepfakeMAE has a slight decrease ($99.0\% \leftarrow 98.7\%$) in terms of the average accuracy, we highlight that the cross-dataset performance of DeepfakeMAE in Table 1 significantly surpasses that of HCIL [14] by 7.3% on Celeb-DF and by 6% on DFDC datasets. Overall, DeepfakeMAE owns satisfactory intra-dataset detection performance in addition to state-of-the-art cross-dataset detection performance, benefiting from the mechanism that learns robust features from masking and

reconstructing facial parts.

4.4. Ablation Study

Influence of the masking ratio. It is essential to evaluate the influence of the masking ratio, which determines how much areas of the face are masked out. we investigate how the masking ratio affects generalization. We treat Celeb, WildDeepfake, DFDC as the unseen datasets, and the models are trained on FaceForensics++ with different masking ratios.

Note that instead of defining the masking ratio as the ratio of masked area to the entire face, we define the masking ratio as the ratio of masked area to the corresponding facial parts. In this way, if the masking ratio is 50%, for example, then half of the pixels are masked for the selected facial parts that we defined in the masking strategy in Sec. 3.1. Using a simple masking ratio for the entire face could, for example, result in masking of the entire nose, which we do not want. This is because removing a part entirely could prevent the model from learning the consistency among the three facial parts.

In Table 4, we observe that DeepfakeMAE scales well with the masking ratio of 50%. The performance gets a slight drop in the masking ratio of 25%. That is, a low masking ratio causes disadvantages in learning robust features. When the mask rate is 75%, the detection performance is also degraded. That may be because that high masking ratio can raise the difficulty of reconstructing faces. If both real faces and fake faces are not reconstructed well, the distinction between them can be reduced. Therefore, we set masking ratio as 50% in the experiments.

Influence of the masking strategy. We modify the masking strategy in MAE [16] to improve the generalization. To evaluate the effectiveness of the modification, we compare the proposed strategy with that of MAE [16]. Furthermore, since the modified strategy randomly selects parts to mask, evaluating the effects of different masked parts is important. Specifically, without changing the second stage, we implement cross-dataset experiments with different mask strategies in the first stage.

The 2th column and 6th column results in Table 5 demonstrate that modifying the masking strategy of MAE

Table 5. Ablation study - The cross-dataset detection performance (AUC %) of different mask strategies on Celeb-DF, WildDeepfake, and DFDC datasets. Random pixels strategy proposed in [16], cheek & nose, random parts of the proposed DeepfakeMAE are represented as RP [16], C & N, and RA, respectively.

Dataset	RP [16]	Eye	C & N	Lips	RA
Celeb-DF	80.1	82.5	82.1	83.4	**86.3**
WildDeepfake	77.6	78.9	78.1	79.7	**81.8**
DFDC	70.4	72.9	72.5	73.5	**75.2**

Table 6. Ablation study - The cross-dataset detection performance (AUC %) of two branches and meta-learning mode in the second stage on Celeb-DF, WildDeepfake, and DFDC datasets. Finetuning Network and Mapping Network are represented by F branch and M branch, respectively.

Dataset	F branch	M branch	w/o meta	Two branches
Celeb-DF	78.3	77.8	84.3	**86.3**
WildDeepfake	75.4	73.5	80.4	**81.8**
DFDC	74.3	70.1	72.1	**75.2**

[16] can improve the detection performance. The strategy of the 3th, 4th and 5th columns select eye areas, cheek & nose areas and lips areas to patch, showing a performance degradation than that of the proposed random strategy. Meanwhile, all these mask facial parts count for Deepfake video detection. Therefore, the proposed strategy illustrated in Algorithm 1 that focuses on all facial parts is more robust than the strategy that focuses on a certain part only.

Influence of the two branches and meta-learning mode in the second stage. In the second stage, we combine the two branches of (a) Finetuning Network and (b) Mapping Network for cross-dataset detection. To validate the cross-dataset detection performance of each branch, we compare the performance of a single branch with that of two branches. Besides, the Mapping Network uses a meta-learning module to improve the domain generalization. We also construct experiments to evaluate the effectiveness of the module.

First, we detect the videos by using the Finetuning Network, and the results are shown in the 2th column of Table 6. Second, we only implement the branch of Mapping Network to detect videos, and show the results in the 3th column. Third, we combine the two branches and remove the meta-learning module to carry out experiments, and the results are shown in the 4th column of Table 6. The 5th column shows the results of the proposed method that averages the outputs of each branch and utilizes the meta-learning mode in the Mapping Network. We can see that combining two branches achieves better results than using only one
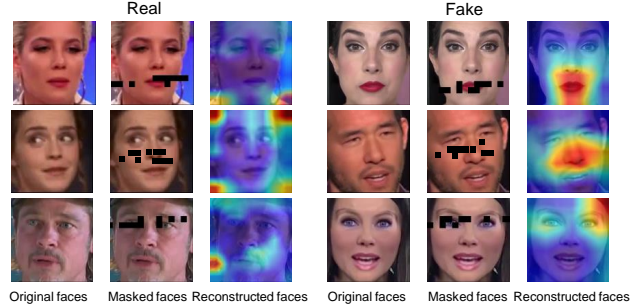

Figure 3. The visualization of DeepfakeMAE. For the fake face, the masked areas (eyes, cheek & nose, lips) are activated. For the real face, the background areas are activated rather than the masked areas.

of the two branches. That is because each branch plays a role in Deepfake detection and combining two branches can improve the performance. Specifically, the Finetuning Network can expose inconsistent features by utilizing the encoder of the first stage. The Mapping Network can reveal the inconsistencies by developing the decoder of the first stage. The fusion of two branches can magnify the distinction between real videos and fake videos and thus improve the cross-dataset detection performance. Moreover, the results in the 4th and 5th columns show that the method with meta-learning achieves better results than that of without meta-learning, which demonstrates that the meta-learning approach can simulate cross-domain detection in the training phase, improving cross-dataset detection performance.

Visualizations. In order to explore the features extracted by the proposed DeepfakeMAE, we generate Class Activation Maps (CAM). Specifically, we utilize the trained model to mask faces and visualize reconstructed faces. As shown in Fig. 3, the activation areas of real and fake faces are different. For the fake face, the facial parts (eyes, cheek & nose, lips) are masked. Due to the lack of consistency, the fake face is reconstructed with some perturbations. After visualizing the features of the network, the masked areas of the reconstructed faces are activated, exposing the inconsistencies of fake faces. For the real face, we also mask the facial parts (eyes, cheek & nose, lips). The consistency of the real face guides the reconstruction, which makes the network can not extract the abnormal inconsistencies. Therefore, there are activation areas in the background areas rather than masked areas. That is, the proposed DeepfakeMAE can detect videos by extracting the facial part consistencies.

5. Conclusion

This paper addresses the Deepfake detection, especially for detecting unseen types of fake videos. By focusing equally on all facial parts rather than relying on specific facial parts, our two-stage model can learn robust representa-

tions based on the consistency of facial parts that only exist on real faces. In the first stage, the model is trained to reconstruct the entire image from a partially masked image of the face in order to learn a robust representation of real images. In the second stage, the model is trained to maximize the discrepancy between real and fake videos. Extensive experiments illustrate the robustness and generalizability of DeepfakeMAE on benchmark datasets.

References

[1] Darius Afchar, Vincent Nozick, Junichi Yamagishi, and Isao Echizen. Mesonet: a compact facial video forgery detection network. In *WIFS*, pages 1–7, 2018. 1, 3

[2] Junyi Cao, Chao Ma, Taiping Yao, Shen Chen, Shouhong Ding, and Xiaokang Yang. End-to-end reconstruction-classification learning for face forgery detection. In *CVPR*, pages 4113–4122, 2022. 1, 3, 6

[3] Lucy Chai, David Bau, Ser-Nam Lim, and Phillip Isola. What makes fake images detectable? understanding properties that generalize. In *ECCV*, pages 103–120. Springer, 2020. 1

[4] Liang Chen, Yong Zhang, Yibing Song, Lingqiao Liu, and Jue Wang. Self-supervised learning of adversarial example: Towards good generalizations for deepfake detection. In *CVPR*, pages 18710–18719, 2022. 1, 3, 6

[5] Umur Aybars Ciftci, Ilke Demir, and Lijun Yin. Fakecatcher: Detection of synthetic portrait videos using biological signals. *IEEE TPAMI*, pages 1–1, 2020. 3

[6] DeepFakes. Accessed october 10, 2018. https://github.com/deepfakes/faceswap, 2018. 2, 5

[7] Brian Dolhansky, Joanna Bitton, Ben Pflaum, Jikuo Lu, Russ Howes, Menglin Wang, and Cristian Canton Ferrer. The deepfake detection challenge (DFDC) dataset. *arXiv preprint arXiv:2006.07397*, 2020. 2, 3, 5

[8] Alexey Dosovitskiy, Lucas Beyer, Alexander Kolesnikov, Dirk Weissenborn, Xiaohua Zhai, Thomas Unterthiner, Mostafa Dehghani, Matthias Minderer, Georg Heigold, Sylvain Gelly, et al. An image is worth 16x16 words: Transformers for image recognition at scale. In *ICLR*, 2021. 4

[9] FaceSwap. Accessed october 29, 2018. https://github.com/MarekKowalski/FaceSwap/, 2018. 2, 5

[10] Christoph Feichtenhofer, Haoqi Fan, Yanghao Li, and Kaiming He. Masked autoencoders as spatiotemporal learners. In *NeurIPS*, 2022. 3

[11] Peng Gao, Teli Ma, Hongsheng Li, Jifeng Dai, and Yu Qiao. Convmae: Masked convolution meets masked autoencoders. In *NeurIPS*, 2022. 3

[12] Zhihao Gu, Yang Chen, Taiping Yao, Shouhong Ding, Jilin Li, Feiyue Huang, and Lizhuang Ma. Spatiotemporal inconsistency learning for deepfake video detection. In *ACM MM*, pages 3473–3481, 2021. 1, 2, 7

[13] Zhihao Gu, Yang Chen, Taiping Yao, Shouhong Ding, Jilin Li, and Lizhuang Ma. Delving into the local: Dynamic inconsistency learning for deepfake video detection. In *AAAI*, volume 36, pages 744–752, 2022. 2, 3

[14] Zhihao Gu, Taiping Yao, Yang Chen, Shouhong Ding, and Lizhuang Ma. Hierarchical contrastive inconsistency learning for deepfake video detection. In *ECCV*, pages 596–613. Springer, 2022. 1, 2, 6, 7

[15] Alexandros Haliassos, Konstantinos Vougioukas, Stavros Petridis, and Maja Pantic. Lips don't lie: A generalisable and robust approach to face forgery detection. In *CVPR*, pages 5039–5049, 2021. 1, 3, 6

[16] Kaiming He, Xinlei Chen, Saining Xie, Yanghao Li, Piotr Dollár, and Ross Girshick. Masked autoencoders are scalable vision learners. In *CVPR*, pages 16000–16009, 2022. 2, 3, 4, 7, 8

[17] Kaiming He, Xiangyu Zhang, Shaoqing Ren, and Jian Sun. Deep residual learning for image recognition. In *CVPR*, pages 770–778, 2016. 5

[18] Juan Hu, Xin Liao, Jinwen Liang, Wenbo Zhou, and Zheng Qin. FInfer: Frame inference-based deepfake detection for high-visual-quality videos. In *AAAI*, volume 36, pages 951–959, 2022. 1, 6

[19] Juan Hu, Xin Liao, Wei Wang, and Zheng Qin. Detecting compressed deepfake videos in social networks using frame-temporality two-stream convolutional network. *IEEE TCSVT*, 32(3):1089–1102, 2021. 3

[20] Yunpei Jia, Jie Zhang, and Shiguang Shan. Dual-branch meta-learning network with distribution alignment for face anti-spoofing. *IEEE TIFS*, 17:138–151, 2021. 5

[21] Tero Karras, Samuli Laine, and Timo Aila. A style-based generator architecture for generative adversarial networks. In *CVPR*, pages 4401–4410, 2019. 3

[22] Xiaohua Lei, Xiuhua Jiang, and Caihong Wang. Design and implementation of a real-time video stream analysis system based on ffmpeg. In *2013 Fourth World Congress on Software Engineering*, pages 212–216, 2013. 5

[23] Jiaming Li, Hongtao Xie, Jiahong Li, Zhongyuan Wang, and Yongdong Zhang. Frequency-aware discriminative feature learning supervised by single-center loss for face forgery detection. In *CVPR*, pages 6458–6467, 2021. 1, 6

[24] Lingzhi Li, Jianmin Bao, Ting Zhang, Hao Yang, Dong Chen, Fang Wen, and Baining Guo. Face x-ray for more general face forgery detection. In *CVPR*, pages 5001–5010, 2020. 1, 6

[25] Xiaodan Li, Yining Lang, Yuefeng Chen, Xiaofeng Mao, Yuan He, Shuhui Wang, Hui Xue, and Quan Lu. Sharp multiple instance learning for deepfake video detection. In *ACM MM*, pages 1864–1872, 2020. 1, 7

[26] Yuezun Li, Ming-Ching Chang, and Siwei Lyu. In ictu oculi: Exposing ai created fake videos by detecting eye blinking. In *WIFS*, pages 1–7, 2018. 1

[27] Yuezun Li and Siwei Lyu. Exposing Deepfake videos by detecting face warping artifacts. In *CVPRW*, pages 46–52, 2019. 3, 6

[28] Yuezun Li, Xin Yang, Pu Sun, Honggang Qi, and Siwei Lyu. Celeb-DF: A large-scale challenging dataset for deepfake forensics. In *CVPR*, pages 3207–3216, 2020. 2, 3, 5

[29] Honggu Liu, Xiaodan Li, Wenbo Zhou, Yuefeng Chen, Yuan He, Hui Xue, Weiming Zhang, and Nenghai Yu. Spatial-phase shallow learning: rethinking face forgery detection in

frequency domain. In *CVPR*, pages 772–781, 2021. 1, 2, 3, 6

[30] Ilya Loshchilov and Frank Hutter. Decoupled weight decay regularization. *arXiv preprint arXiv:1711.05101*, 2017. 5

[31] Iacopo Masi, Aditya Killekar, Royston Marian Mascarenhas, Shenoy Pratik Gurudatt, and Wael AbdAlmageed. Two-branch recurrent network for isolating deepfakes in videos. In *ECCV*, pages 667–684, 2020. 3

[32] Trisha Mittal, Uttaran Bhattacharya, Rohan Chandra, Aniket Bera, and Dinesh Manocha. Emotions don't lie: An audio-visual deepfake detection method using affective cues. In *ACMMM*, pages 2823–2832, 2020. 1, 3

[33] Aakash Varma Nadimpalli and Ajita Rattani. On improving cross-dataset generalization of deepfake detectors. In *CVPR*, pages 91–99, 2022. 1

[34] Huy H Nguyen, Junichi Yamagishi, and Isao Echizen. Capsule-forensics: Using capsule networks to detect forged images and videos. In *ICASSP*, pages 2307–2311, 2019. 1

[35] Yuval Nirkin, Yosi Keller, and Tal Hassner. Fsgan: Subject agnostic face swapping and reenactment. In *ICCV*, pages 7184–7193, 2019. 3

[36] Yuyang Qian, Guojun Yin, Lu Sheng, Zixuan Chen, and Jing Shao. Thinking in frequency: Face forgery detection by mining frequency-aware clues. In *ECCV*, pages 86–103, 2020. 1, 3

[37] Andreas Rossler, Davide Cozzolino, Luisa Verdoliva, Christian Riess, Justus Thies, and Matthias Nießner. Faceforensics++: Learning to detect manipulated facial images. In *ICCV*, pages 1–11, 2019. 1, 2, 5, 7

[38] Ekraam Sabir, Jiaxin Cheng, Ayush Jaiswal, Wael AbdAlmageed, Iacopo Masi, and Prem Natarajan. Recurrent convolutional strategies for face manipulation detection in videos. *Interfaces (GUI)*, 3(1):80–87, 2019. 1

[39] S Sharma, Karthikeyan Shanmugasundaram, and Sathees Kumar Ramasamy. Farec-cnn based efficient face recognition technique using dlib. In *ICACCCT*, pages 192–195, 2016. 6

[40] Ke Sun, Hong Liu, Qixiang Ye, Yue Gao, Jianzhuang Liu, Ling Shao, and Rongrong Ji. Domain general face forgery detection by learning to weight. In *AAAI*, volume 35, pages 2638–2646, 2021. 1, 6

[41] Ke Sun, Hong Liu, Qixiang Ye, Yue Gao, Jianzhuang Liu, Ling Shao, and Rongrong Ji. Domain general face forgery detection by learning to weight. In *AAAI*, volume 35, pages 2638–2646, 2021. 3

[42] Justus Thies, Michael Zollhöfer, and Matthias Nießner. Deferred neural rendering: Image synthesis using neural textures. *ACM TOG*, 38(4):1–12, 2019. 2, 5, 7

[43] Justus Thies, Michael Zollhofer, Marc Stamminger, Christian Theobalt, and Matthias Nießner. Face2face: Real-time face capture and reenactment of rgb videos. In *CVPR*, pages 2387–2395, 2018. 2, 5

[44] Zhan Tong, Yibing Song, Jue Wang, and Limin Wang. Videomae: Masked autoencoders are data-efficient learners for self-supervised video pre-training. In *NeurIPS*, 2022. 3

[45] Sheng-Yu Wang, Oliver Wang, Richard Zhang, Andrew Owens, and Alexei A Efros. Cnn-generated images are surprisingly easy to spot... for now. In *CVPR*, pages 8695–8704, 2020. 1, 2, 6

[46] Zhi Wang, Yiwen Guo, and Wangmeng Zuo. Deepfake forensics via an adversarial game. *IEEE TIP*, 31:3541–3552, 2022. 1

[47] Haiwei Wu, Jiantao Zhou, Jinyu Tian, Jun Liu, and Yu Qiao. Robust image forgery detection against transmission over online social networks. *IEEE TIFS*, 17:443–456, 2022. 1

[48] Xin Yang, Yuezun Li, and Siwei Lyu. Exposing deep fakes using inconsistent head poses. In *ICASSP*, pages 8261–8265, 2019. 1, 2

[49] Egor Zakharov, Aliaksandra Shysheya, Egor Burkov, and Victor Lempitsky. Few-shot adversarial learning of realistic neural talking head models. In *ICCV*, 2019. 3

[50] Hanqing Zhao, Wenbo Zhou, Dongdong Chen, Tianyi Wei, Weiming Zhang, and Nenghai Yu. Multi-attentional deepfake detection. In *CVPR*, pages 2185–2194, 2021. 1, 2, 6

[51] Wanyi Zhuang, Qi Chu, Zhentao Tan, Qiankun Liu, Haojie Yuan, Changtao Miao, Zixiang Luo, and Nenghai Yu. Uia-vit: Unsupervised inconsistency-aware method based on vision transformer for face forgery detection. In *ECCV*, 2022. 1, 2

[52] Bojia Zi, Minghao Chang, Jingjing Chen, Xingjun Ma, and Yu-Gang Jiang. WildDeepfake: A challenging real-world dataset for deepfake detection. In *ACMMM*, pages 2382–2390, 2020. 2, 3, 5, 6, 7